energies

MDPI

Article

Fault Detection in HVDC System with Gray Wolf Optimization Algorithm Based on Artificial Neural Network

Raad Salih Jawad * and Hafedh Abid

Laboratory of Sciences and Techniques of Automatic Control & Computer Engineering (Lab-STA) Sfax, National School of Engineering of Sfax, University of Sfax, Sfax 3029, Tunisia
* Correspondence: raad.saleh@gmail.com; Tel.: +964-771-338-1461

Abstract: Various methods have been proposed to provide the protection necessitated by the high voltage direct current system. In this field, most of the research is confined to various types of DC and AC line faults and a maximum of two switching converter faults. The main contribution of this study is to use a new method for fault detection in HVDC systems, using the gray wolf optimization method along with artificial neural networks. Under this method, with the help of faulted and non-faulted signals, the features of the voltage and current signals are extracted in a much shorter period of the signal. Subsequently, differences are detected with the help of an artificial neural network. In the studied HVDC system, the behavior of the rectifier, along with its controllers and the required filters are completely modeled. In this study, other methods, such as artificial neural network, radial basis function, learning vector quantization, and self-organizing map, were tested and compared with the proposed method. To demonstrate the performance of the proposed method the accuracy, sensitivity, precision, Jaccard, and F1 score were calculated and obtained as 99.00%, 99.24%, 98.74%, 98.00%, and 98.99%, respectively. Finally, according to the simulation results, it became evident that this method could be a suitable method for fault detection in HVDC systems.

Keywords: artificial neural network; fault detection; HVDC; gray wolf optimization

Citation: Jawad, R.S.; Abid, H. Fault Detection in HVDC System with Gray Wolf Optimization Algorithm Based on Artificial Neural Network. *Energies* **2022**, *15*, 7775. https://doi.org/10.3390/en15207775

Academic Editor: Ali Farzamnia

Received: 13 September 2022
Accepted: 19 October 2022
Published: 20 October 2022

1. Introduction

Due to their lower cost over long distances and their ability to transmit more power, high voltage direct current (HVDC) transmission systems have been widely used for power transmission projects with overhead transmission lines, bulk power, and asynchronous connections. Issues such as the long distance of the lines, the environments of the transmission lines, and adverse weather conditions in HVDC transmission lines have resulted in an increased error rate [1,2].

Currently, protection systems based on traveling waves and voltage derivatives are typically used as the main protection, as well as current differential protection and DC voltage reduction as backup protections for HVDC transmission lines. Protections based on traveling waves and voltage derivatives are sensitive to fault resistance and misdiagnose in detecting high impedance faults, as they use the rate of the voltage change to detect the fault. In addition, current differential protection has a relatively slow performance, due to the transmission line's charge and discharge currents. The main DC voltage reduction has low reliability in detecting faults inside and outside the protection zone [1,2]. Therefore, developing new protection schemes with better performance for HVDC transmission lines is necessary.

With the expansion of applications in AC/DC systems, the expectation of reliability in high-voltage direct current systems has increased dramatically. There are numerous advantages of these systems, such as no interference during transmission, the ability to connect two networks with different frequencies, and the selection of the optimal frequency according to the maximum efficiency of power plants for long distances, as well as high power transmission capacity and having two or more network connections [3,4].

An early diagnosis of a fault site allows for faster repair. Faults can cause consumers to lose electricity for short or long periods, causing significant financial loss, especially in industries. These flaws must be identified quickly to keep a power system stable. The problem of detecting a fault has long captivated engineers and researchers. So far, research has focused on locating transmission line defects. Defects in transmission lines affect power systems more than faults in sub-transmission and distribution systems, and physical inspection of transmission lines takes longer. The purpose of fault-finding is to find the exact location of the issue. Secondary protection equipment often uses fault location algorithms to determine the fault's location. Furthermore, transmission line faults may be temporary or permanent. Overhead lines have several self-clearing transient faults [5]. As a result, the power supply is not permanently interrupted.

A permanent failure can be identified and de-energized using circuit breakers connected to the protective relaying equipment. The power supply can be restored as soon as the repair personnel finish their work. The complete line must be inspected if the problem is not precisely recognized. The problem must be known, or at least substantially known, to effectively investigate the defect. Faster power restoration reduces inspection time and maintenance costs and provides improved service. This way, power outages can be prevented.

On the other hand, temporary faults are vital, since they can self-clear and do not permanently affect the supply. The location of the fault can be used to find cable weaknesses. Thus, preventative maintenance programs can be devised [6].

As the distribution networks and the power used by customers are both AC, using AC TL saves money on inverters and rectifiers. DC TL is required when transmission distances and power requirements increase. A DC system is the only way to connect two AC systems with different frequencies. HVDC technology is used to transport power between non-synchronized AC networks. As DC transmission lines have no skin effect, the inductive and capacitive properties of HVDC systems are unaffected. Using quick DC power modulation, the HVDC control system can limit power oscillations in connected AC power grids. This technique improves transient system stability. Foot patrols with various mobility methods and binoculars can locate faults by visual observation and assessments. However, it takes a long time to investigate a poor line.

There has been a growth in the number of algorithms designed to find faults in power systems in recent years, allowing for better protection and easier maintenance. The following are commonly used ways for locating faults in current systems:

1. The analytical method, which relies on fundamental frequency measurements, such as impedance.
2. In the so-called traveling wave techniques, an electrical pulse is sent along the wire, and the reflected signals are recorded at both ends. The distance to the fault site can be determined by the pulse's return time after passing through the fault site.
3. Approaches that use electrical magnitudes at fundamental frequencies capture voltage and/or current alerts on the ends of a considered road and find its periodic fundamental factor before and after the fault. If these crucial elements are handled properly, the error can be located.
4. Knowledge-based techniques.

Artificial Intelligence, which is a subfield of computer science, studies how machines may emulate human thought and behavior. The field of AI encompasses numerical and non-numerical computations and symbolic computations.

Artificial intelligence involves making rational decisions and having the ability to deal with incomplete information, adapt to new circumstances throughout time, and improve each passing day.

Modern power system automation and control are said to employ three key families of artificial intelligence (AI) techniques:

1. Expert systems.
2. Synthetic neuronal systems.
3. Systems of fuzzy logic.

There is much potential for neural network research in control systems, fault detection, pattern categorization, and load forecasting in power systems, and so on. Neural networks can learn, generalize and tolerate faults, and may be used in a networked setting.

Faults on HVDC transmission lines (TL) can be detected, classified, and located using the gray wolf optimization (GWO) algorithm based on an artificial neural network (ANN).

The gray wolf optimization method selects the best features, which are then used to train the neural network.

The following features are some of the study's main contributions:

1. The faults in the HVDC TL connection are the focus of this study, as most of the previous research has focused on the AC grid, rectifier, or inverter stations.
2. The GWO algorithm, based on ANN, is used to pinpoint the location of faults in this study, which includes a process of detection and classification. Most prior studies on this topic have focused on identifying and characterizing problems.
3. Instead of working in an offline environment, the GWO algorithm, based on ANN, in the HVDC approach allows you to acquire results in an online context. Instantaneous and permanent HVDC faults may be detected by utilizing the GWO algorithm, based on ANN, to diagnose HVDC problems, while any other method in offline conditions can only detect permanent faults.
4. Using the GWO algorithm, based on ANN, eliminates the need for voltage and current monitoring equipment required at converter stations, necessary for any HVDC system.

Fault detection is the starting unit of the protection block. So, a fast and reliable method needs to detect the faults in HVDC protection systems. In this study, AI is used to get a fast response to fault detection. Actually, the AI algorithm needs time to learn, but after the learning step, the trained network is used for fault detection. In the testing step, fault detection by AI is very much faster than the logic algorithms.

The rest of the paper is organized into six sections. Section 2 includes a literature review. Section 3 includes the materials and methodologies for the HVDC fault detection method used in the proposed system. Section 4 describes the implementation of the selected methodology, illustrates the methods, and includes the analysis of the model. Section 5 discusses the proposed algorithm within the proposed system and analyzes it under various conditions. Lastly, Section 6 discusses the conclusion and future scope of the research.

2. Literature Review

The protection of HVDC converters has been the subject of much research. The first attempt was made by Kandil using classification algorithms in HVDC [7]. In this study, three types of neural networks were used, and comparisons were made among them. In [8], the radial basis function (RBF) neural network was used for fault detection in an HVDC sample system.

This study used a classifier to reduce preprocessing data before entering the information into the neural network. A new scheme for reducing neural simulation data for neural network training used in HVDC monitoring is presented in [9]. Shang et al. [10] proposed a wavelet-based fault detection technique to protect the HVDC system. In [11], MR analysis of wavelet transform was used to extract important features of fault data for HVDC monitoring. Reference [12] used wavelet transform for HVDC protection.

Most studies [13–17] focus on the selection of the control function to provide the required protection, but, in separating the types of converter faults, a maximum of two types of converter faults are simulated and divided into steps: AC, DC fault, and converter fault. While controlling the performance of individual converters, thyristor valves can provide higher degrees of protection against DC and AC line faults as well as internal converter faults.

In [14], they used the wavelet transform to extract the feature of the fault. The three features of their method are the root means: the inverter's wavelet energy spectrum information entropy, wavelet energy skewness, and wavelet detail coefficients squared values.

Wang et al. proposed a new long short-term memory (LSTM) method for fault detection and classification [15]. They compared their method with bidirectional LSTM and convolutional neural networks and observed that the LSTM has a lower processing time and obtains 100% accurate results.

The bidirectional Gated Recurrent Unit was proposed in [16] for feature extraction on the bidirectional structure. With this method, detailed information and features are extracted and used to classify faults.

The discrete Fourier transform, based on the decision tree, was used in [18] for fault detection and classification. The discrete wavelet transform combined with the decision tree was used in [19] to diagnose faults. In [19], the wavelet transform was combined with S-transform to classify and detect the fault in grid-tied systems. The support vector machine and a naive classifier were used in [20] to declare the type of faults. They used the Hilbert–Huang transform for feature extraction in their work. The discrete wavelet transform, based on the extreme learning machine, was used to detect and classify faults in the microgrid [21]. The semi-supervised fault detection and classification methods were used in [21]. The discrete wavelet transform, based on ANN Taguchi, was used in [22].

The poor architecture used by machine learning and neural network-based methods [23–25] limits the system's ability to learn its complicated non-linear properties. Due to the abundance of features, most of which are insignificant, these approaches cannot effectively leverage the advantages of numerous features.

One of the most important problems in identifying faults in HVDC systems is that the machine learning systems (in this study, ANNs) with non-main features that do not play an important role in learning neural networks cause errors in learning. To address this problem, this study presents the GWO method to select the best features and uses this feature in the training of the neural network, containing several hidden layers that make it possible to increase classification accuracy by mastering the system's intricate non-linear features.

In this study, the types of faults in HVDC converters are introduced separately for the inverter and rectifier, then, using MATLAB software, the simulation and dynamic behavior of the rectifier, together with the relevant controller, are investigated. Then, using the GWO, the best features are determined, and the potential neural network is trained by extracting the properties of the best features of the fault signal and the original data. This way, the types of faults related to converters are distinguished from each other. Finally, to validate the results, a comparison of the test data output for the multilayer perceptron (MLP), radial basis function (RBF), learning vector quantization (LVQ), and self-organizing map (SOM) are given.

3. Materials and Methods

In this study, faulted and non-faulted signals were created to analyze HVDC fault detection. For this purpose, multiple signals with different types of AC and DC faults were created. The 12 features that depend on the voltage, current, and their components are extracted from these signals. Some of these features are unsuitable for the training of ANN [26,27], and using these features would result in errors and reduce detection accuracy. For this reason, the best and the most accurate features should be selected. Thus, the GWO method, first presented in [28], was used for the feature selection.

The summary of the proposed method is shown in Figure 1.

As seen in Figure 1, the 13 faulted signals containing the AC and DC faulted signals were created manually by Simulink-MATLAB. Then, for each fault, the output signals were obtained. These signals contain a huge number of features, most of which are not suitable for training the neural network, and sometimes they can make mistakes in fault detection. For this reason, the best and most useful features have to be selected to train the network. The GWO method was used to select the best features, and these features were used to train the neural network. The GWO method scenario is shown on the right side of the flowchart.

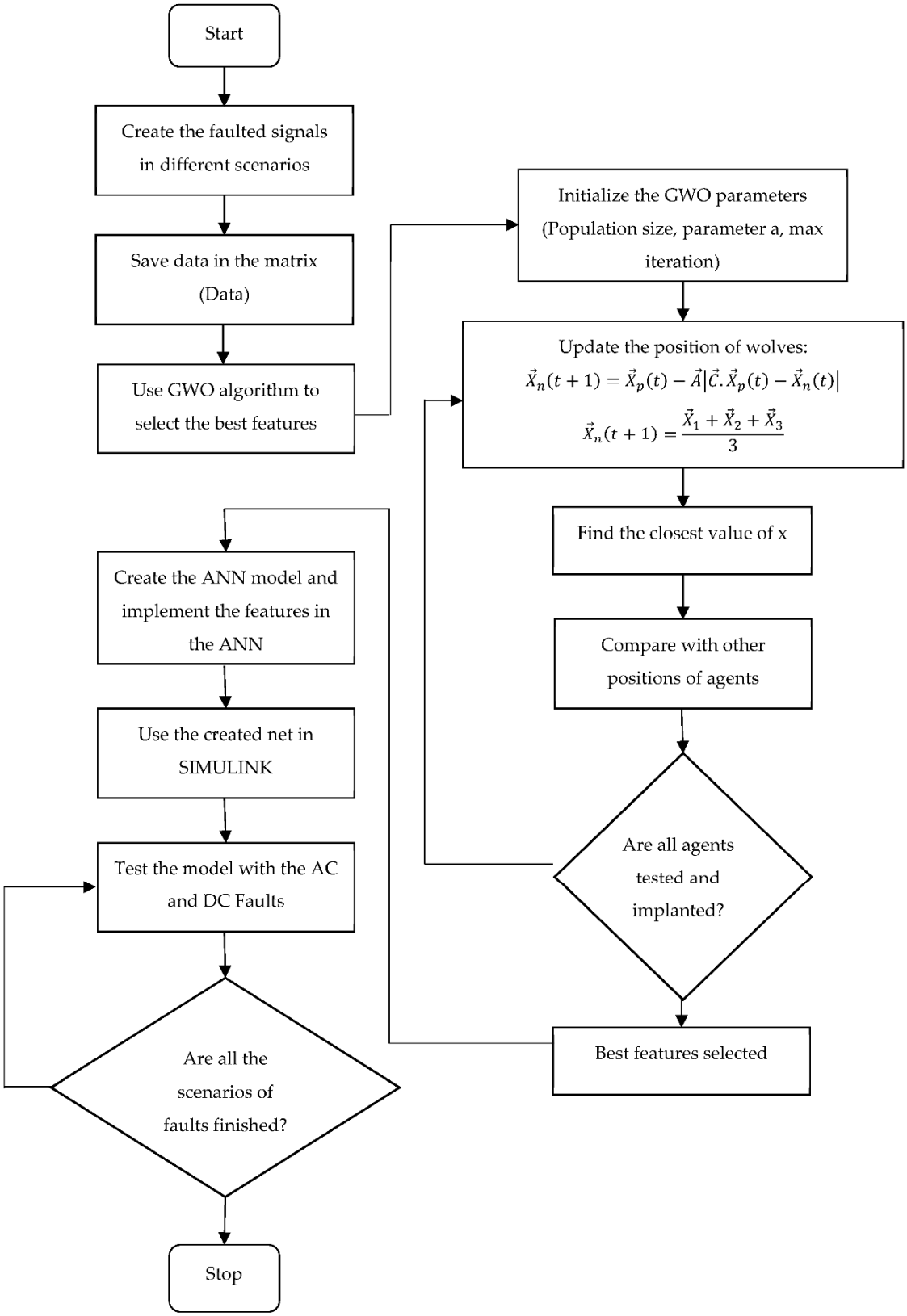

Figure 1. Summary of the proposed method for HVDC fault detection.

Primarily, the GWO performs by mimicking grey wolves' leadership hierarchy and hunting mechanisms, which they exhibit in the natural environment. Four grey wolf types exist in each pack, namely, the alpha, beta, delta, and omega. Moreover, their hunting

process comprises three stages: searching, encircling, and attacking the prey, which are also performed during the optimization process. As Mirjalili suggests, GWO is a novel and robust meta-heuristic method [28]. It is also an easy-to-understand and feasible-to-implement algorithm because it is natural and animal-inspired. The main advantage of GWO is that it is adaptable, easy, and plain. A few recent studies have shown that GWO may provide satisfying results when compared to other popular and successful meta-heuristic concepts. For example, Mirjalili compared GWO with the gravitational search algorithm (GSA), differential evolution (DE), PSO, evolution strategy, and evolutionary programming through 29 test functions.

The hierarchy of the gray wolves is shown in Figure 2.

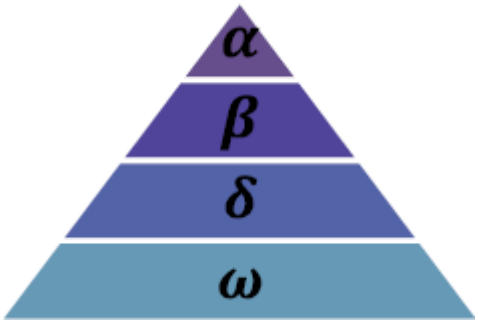

Figure 2. Hierarchy of the gray wolf.

The wolves' social hierarchy is mathematically modeled to solve any problem of optimization that requires the best solution, which is called alpha (α). The second and third best solutions are termed beta (β) and delta (δ), and other solutions are termed omega (ω).

The GWO method selects the best features from the voltage, current, and derivatives, which are then used to train the neural network. ANN is a numerical representation of the ANNs in an individual's cerebrum, which are made up of a massive number of nerve cells called neurons linked together. The average number of neurons in a human brain is approximately 10^{11} [29,30].

The effect of contributions to the neuron is altered in ANNs using mathematical properties, which are referred to as loads. Before being conveyed to neurons, each piece of information is duplicated through comparing weight. Then, a neuron aggregates such weighted characteristics, despite the value of any predisposition, and passes the summation results, via actuation work, to determine the neuron's outcome. In addition, the bias values give the neuron more flexibility when changing the output value, depending on the features it needs to detect. When no bias is utilized, the neuron's output is 0 whenever inputs are 0 because the weights are multiplied by such inputs. As a result, the presence of bias value enables neurons to evaluate the needed output depending on the feature [31]. Equation (1) shows the synopsis S of inputs and the bias of neuron j [31].

$$s_j = \sum_i x_i \, w_{ij} + b_j \tag{1}$$

The value x_i represents the contributions of that neuron, w_{ij} are loads to those contributions, and b_j represents the neuron's bias. The visual layout of the way that a neuron grips the contributions to request registering results is shown in Figure 3.

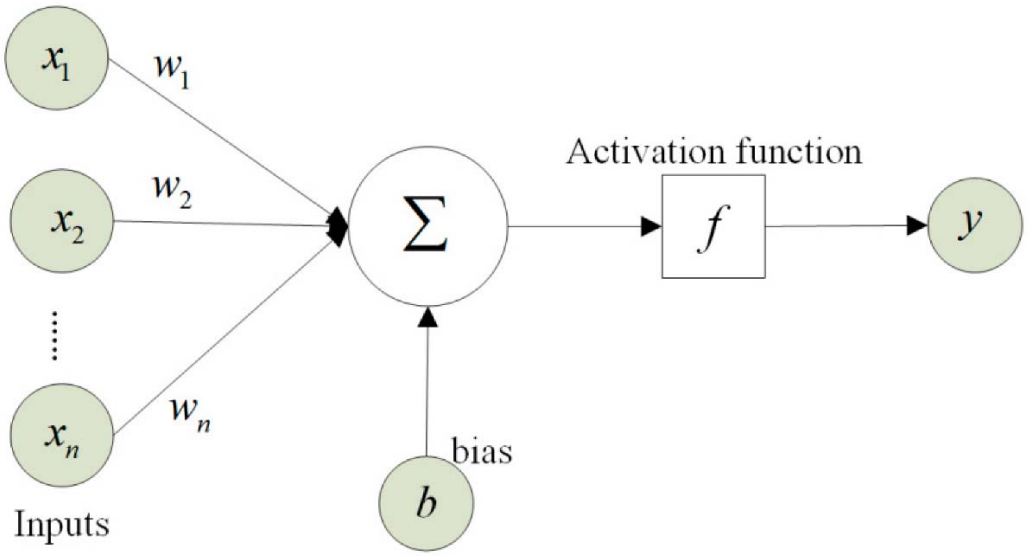

Figure 3. Visual representation of Neuron's Calculation operations [31].

4. Simulink Model

Different models were studied to analyze and identify faults in the HVDC system. The HVDC converter acts on the AC side as the source of current harmonics and voltage harmonics on the DC side. The order of output harmonics depends on the number of converter valves (P), which, for AC current harmonics, is n = kP ± 1, and for DC voltage harmonics is n = kP, and k is an integer. For this purpose, AC filters on both sides of the rectifier and inverter were used to remove the current harmonics on the AC side. In the simulation, to solve the equations of the power system and control/protection system, the sampling time was performed with Ts = 50 µs. The main control of HVDC in this simulation was rectifier control on the rectifier side and power control on the inverter side.

The difference in the characteristics of the thyristors in a valve can cause severe stress during a normal operation. An improper operation of each pole causes a voltage drop on all thyristors of a valve, leading to a sudden decrease in transmitting power. Therefore, the HVDC converter must be protected as a stand-alone device.

The Simulink model for creating the different faults is shown in Figure 4.

Modern HVDC uses Voltage Source Converters (VSC). However, the model used in this study utilized thyristors. There are well-known and advanced protection strategies for thyristor-based two-terminal HVDC systems available in the literature [32–34]. Current protection challenges are related to VSC-based systems, particularly multi-terminal DC systems. In this study, the GWO method, the main subject, was used to evaluate the features and select the best form of voltage and current signal. In future studies, the authors recommend using a VSC-based HVDC system in simulation studies. The Simulink model used the neural network for testing the system is shown in Figure 5, where the trained neural network was used to test the system. This network was trained by the signals obtained from the model created for each fault. All the faults were used to train this network. Thus, neural network inputs used the features of the signals selected by the GWO method. In this study, the protection systems appeared to react to all types of faults. However, any protection algorithm in the HVDC system aimed to operate the relay for internal faults and to make it stable for external faults. The analysis of the system's stability was not the main aim of this paper.

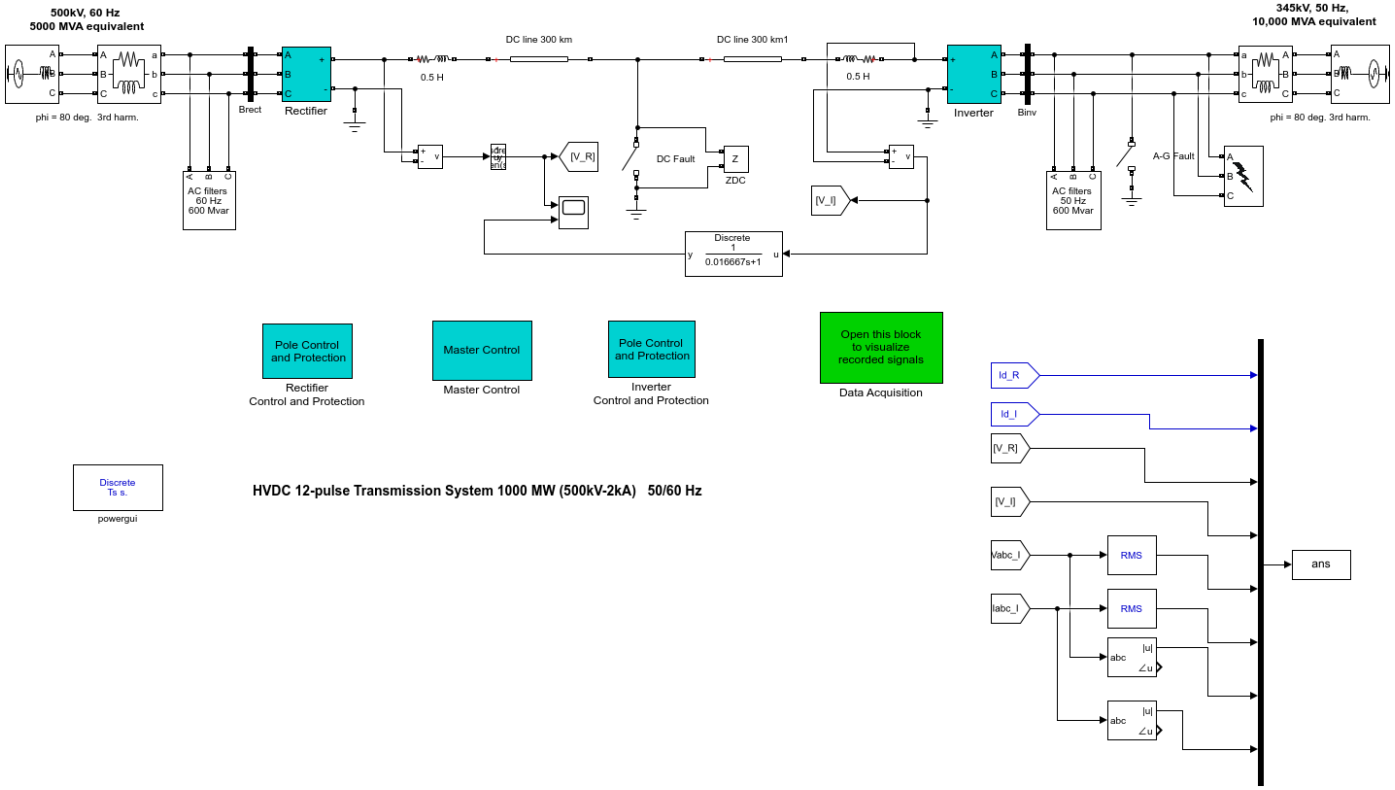

Figure 4. Simulink model for creating the faults.

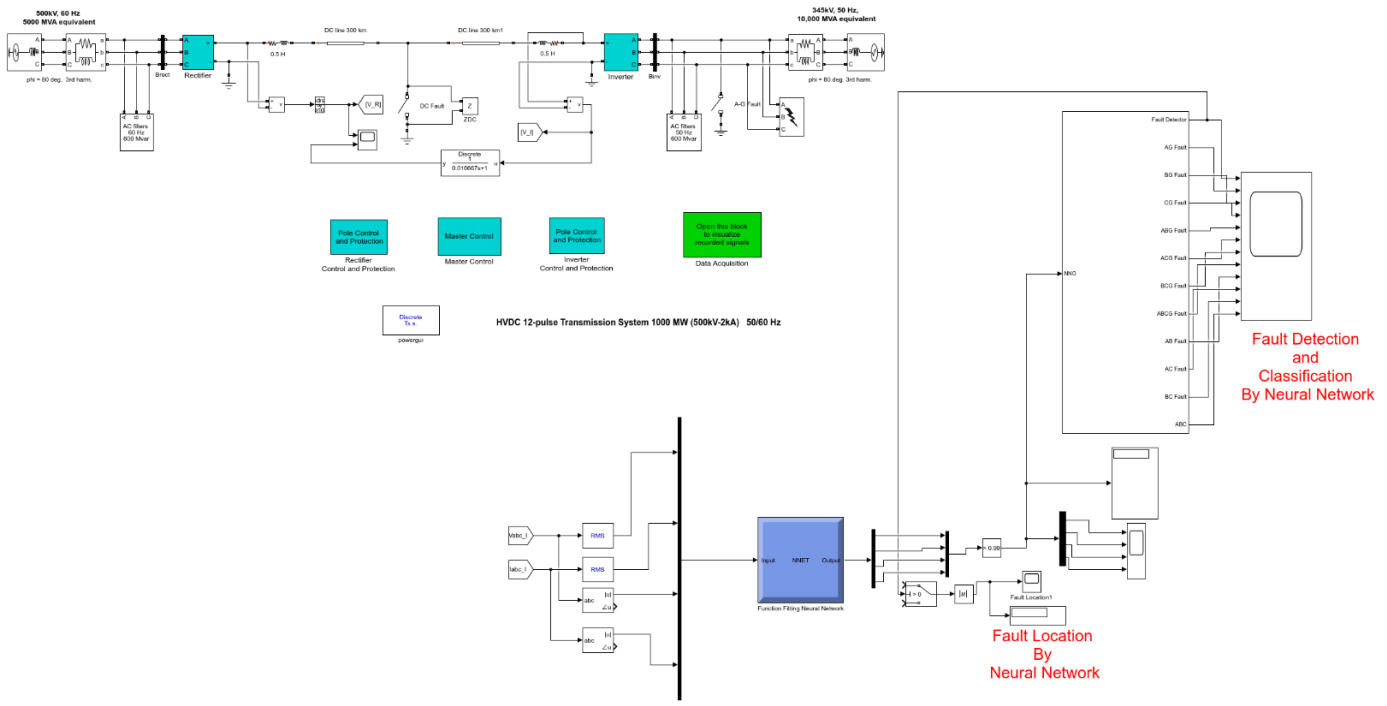

Figure 5. Simulink model using the neural network.

5. Results and Discussion

The proposed fault detection and class method's overall effectiveness are demonstrated in this section, along with individual parameter modifications. Specific values were displayed by the voltage and fault signals in grid-linked and island modes, respectively. Therefore, it became tough to lay out an incorporated fault category scheme. Thus, the

proposed model's performance was analyzed separately for different gadget topologies and working modes.

The criteria of sensitivity, accuracy, F1-score, and precision were utilized to evaluate the suggested approach and were compared to the HVDC fault classification systems. The accuracy percentage in best and worst cases were 0 and 100, and the proximity to the value of 100 indicated high accuracy of the classification algorithm. Equations (2)–(7) show the calculations of accuracy, sensitivity, specificity, precision, Jaccard, and F1 score, respectively [35–37]:

$$Accuracy = \frac{(TP + TN)}{(TP + FP + TN + FN)} = \frac{N_{TD}}{N_{CC}} \quad (2)$$

In this equation, N_{TD} presents the total wide variety of entered facts for the evolved model, and N_{CC} implies the variety of correctly categorized information. The proposed network might function similarly even when the distribution line is relaxed. Table 1 shows the mean accuracy derived for each distribution line. As a result, the proposed classifier's best accuracy was recorded at 99.65% for the grid-related radial mode operation. The classifier performed higher than 99.6% for the other device configurations, which changed in keeping with the expectation.

$$Sensitivity = \frac{TP}{(TP + FN)} \quad (3)$$

$$Specificity = \frac{TN}{(TN + FP)} \quad (4)$$

$$Precision = \frac{TP}{(TP + FP)} \quad (5)$$

$$Jaccard = \frac{TP}{(TP + FP + FN)} \quad (6)$$

$$F1 - Score = 2 \cdot \frac{Precision \cdot Recall}{(Precision + Recall)} \quad (7)$$

Table 1. The average accuracy of the fault detection.

	Average Accuracy (%)
Line one–three	99.23
Line one–two	99.44
Line three–four	99.41
Line three–five	99.52
Line five–six	99.48

The TP (True Positive) index represents the subjects that had the fault classification correctly. TN (True Negative) represents the classifier that detects faults correctly that do not depend on the original signal. FP (False Positive) represents the subjects misidentified as fault signals. FN (False Negative) represents the subjects mistakenly diagnosed as non-fault signals, using the confusion matrix (CM), in which the 11 different fault classes were inserted into the x-axis and y-axis in the form of an 11 by 11 matrix. The vertical ranges symbolized the anticipated flaw elegantly, while the horizontal stages showed the true splendor. The rates of true positives (TP), true negatives (TN), false positives (FP), and false negatives (FN) were also reported in the confusion matrix (CM). The confusion matrix of the proposed classifier is shown in Figure 6.

	a-g	b-g	c-g	ab-g	bc-g	ac-g	a-b	b-c	c-a	abc-g	DC
a-g	495	0	0	5	0	0	0	0	0	0	0
b-g	0	490	0	0	0	0	0	0	0	0	0
c-g	0	0	488	2	0	0	0	0	0	0	0
ab-g	0	0	0	448	0	0	2	0	0	0	0
bc-g	0	0	0	0	497	0	0	0	0	0	3
ac-g	0	0	0	0	0	499	0	0	0	1	0
a-b	0	0	0	2	0	0	476	0	2	0	0
b-c	0	0	0	0	0	0	0	480	0	0	0
c-a	0	0	0	0	0	0	0	0	470	0	0
abc-g	0	0	0	0	0	0	0	0	0	480	0
DC	0	0	0	0	0	0	0	0	0	0	450

Figure 6. Confusion matrix of the proposed classifier.

In system learning, to test the model's overall performance, a listing of the pattern of the records was used to measure the validity of the introduced version, which had to be more specific than the trained records. The current and voltage waveforms for the individual datasets were combined and shuffled to create a total of 1600 samples. To test the efficiency of the suggested model, 35% of the records were then randomly selected. With the help of various system configurations and operating modes, the proposed device's overall performance for strains 1–3 was simulated. This performance was then visualized in Figure 7.

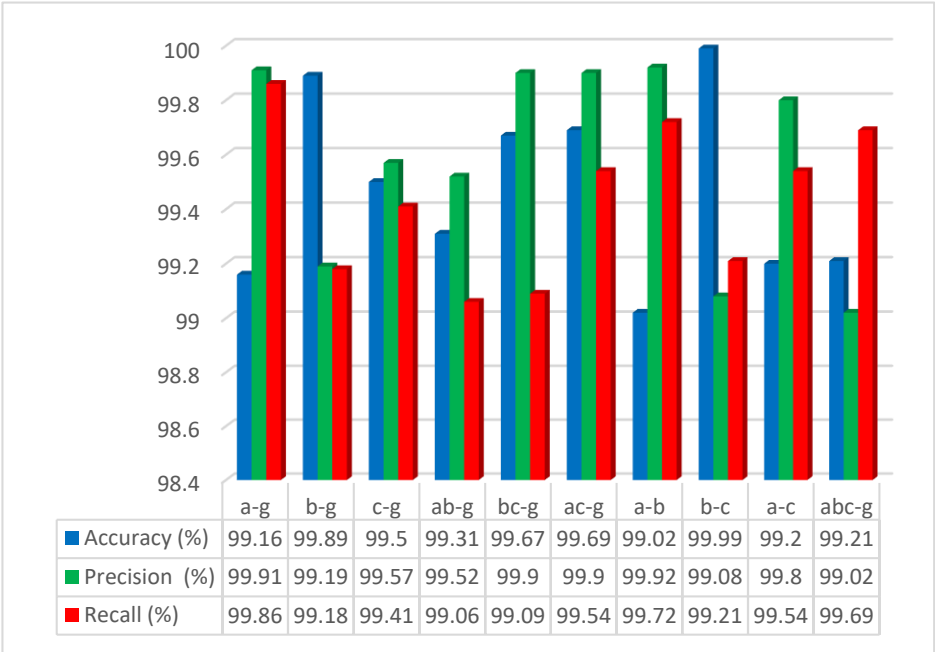

	a-g	b-g	c-g	ab-g	bc-g	ac-g	a-b	b-c	a-c	abc-g
Accuracy (%)	99.16	99.89	99.5	99.31	99.67	99.69	99.02	99.99	99.2	99.21
Precision (%)	99.91	99.19	99.57	99.52	99.9	99.9	99.92	99.08	99.8	99.02
Recall (%)	99.86	99.18	99.41	99.06	99.09	99.54	99.72	99.21	99.54	99.69

Figure 7. Simulation results as a graphic for Accuracy, Precision, and Sensitivity (Recall).

As seen in Figure 6, the system checked the a-g fault 500 times in total and correctly found the fault 495 times. ANN found this type of fault mistily only five times. There were

no faults for b-g, b-c, c-a, abc-g, and DC faults. As a result, this scenario showed that the selected features were the best for training and testing the network.

However, the average accuracy could not provide accurate results about model performance. Therefore, the category's overall performance was evaluated via the F1 score to examine how the classifier behaved for error training. The F1 score parameter represents a feature of precision, sensitivity or recall, and accuracy, considered first-rate when it is equal to 1 and worst when it is equal to 0.

The accuracy, precision, recall, and F1 score results are shown below in Table 2.

Table 2. Accuracy (%), Precision (%), sensitivity (%), and F1-Score results.

Fault Class	Accuracy (%)	Precision (%)	Sensitivity (%)	F1-Score
a-g	99.16	99.91	99.86	99.88
b-g	99.89	99.19	99.18	99.64
c-g	99.50	99.57	99.41	99.84
ab-g	99.31	99.52	99.06	99.46
bc-g	99.67	99.90	99.09	99.30
ac-g	99.69	99.90	99.54	99.23
a-b	99.02	99.92	99.72	99.70
b-c	99.99	99.08	99.21	99.69
a-c	99.20	99.80	99.54	99.02
abc-g	99.21	99.02	99.69	99.66
DC	99.15	99.90	99.93	99.88

The graphical illustration of these results is shown in Figure 7.

The proposed technique extracted features from three-phase current and voltage waveforms with a sampling frequency of 20 kHz. A sampling frequency lower than 20 kHz can be good, because of the restrictions of the information acquisition tool. Therefore, the overall performance of the proposed classifier's fault type was investigated by converting the kind of input signal and the sampling rate. The sampling frequency used in these studies was changed to 5, 10, 15, 20, 25, and 30 kHz, and the kinds of input signals were voltage waveform or current waveform, blended current, and voltage waveform. The effects of sampling frequency and the precise signal were completed by performing the classification technique five times. After that, the average value of the accuracy was determined to acquire the very last effects, as shown in Figure 8.

The increase in accuracy type was expected for a higher sampling frequency, as it carried more precise fault information for an excellent short circuit fault class. Furthermore, combined current and voltage waveforms provided the highest overall performance for all when the sampling frequency was taken into consideration. At a lower sampling rate, a better category performance was found with the three-phase current waveform rather than with the three-phase voltage waveform. Moreover, the proposed gadget was completed with higher voltage signal records and with a better sampling frequency. Between 10 kHz and 20 kHz sampling frequencies, current waveform and blended current and voltage waveform showed nearly identical accuracy types. This scenario was anticipated because the voltage waveform incorporates much less low-frequency fault information than the modern-day waveform for the available fault class. However, the voltage waveform contained temporary mistakes that were appropriate for investigating at a better sampling rate.

The above evaluation suggested that the expected accuracy could not be executed with current or voltage waveforms alone. If each waveform was considered at the same time, a higher chance of faults in overall performance might be seen for the considered frequency degree. From the above study, it was determined that the idea of the use of current or voltage waveforms for the best accuracy classification was shaken. Instead, their fusion gave higher than 99% category accuracy in a large area when frequency range was taken into consideration, which confirmed the performance of the proposed method.

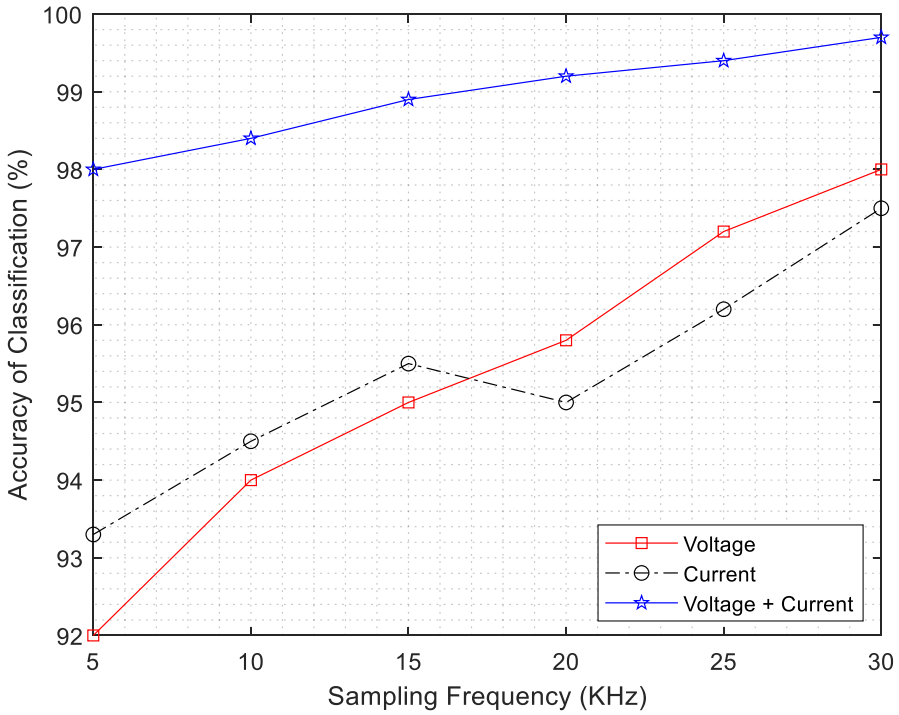

Figure 8. The percentage of the classification accuracy of the proposed method.

Table 3 compares the overall fault classification system for the HVDC fault classification using the proposed method and other methods, in accuracy, sensitivity, precision, Jaccard, and F1 Score.

Table 3. Accuracy, sensitivity, precision, Jaccard, and F1 score of the proposed method.

Method	Accuracy	Sensitivity	Precision	Jaccard	F1 Score	TP	TN	FP	FN
MLP	98.50	98.20	98.80	97.04	98.50	99.02	99.19	1.20	1.81
RBF	96.99	96.99	96.98	94.15	96.99	96.68	96.52	3.01	3.00
LVQ	98.18	98.16	98.17	96.40	98.17	97.23	99.12	1.81	1.82
SOM	92.92	92.89	92.93	86.76	92.91	92.00	92.24	7.00	7.05
Proposed Method	**99.00**	**99.24**	**98.74**	**98.00**	**98.99**	97.20	99.48	1.24	0.74

The proposed method used the GWO method to select the best features from the voltage, current, and their derivatives compared with other neural network architectures, such as multilayer perceptron (MLP), radial basis function (RBF), learning vector quantization (LVQ), and self-organizing map (SOM). The experiments demonstrated that the accuracies of ANN, RBF, LVQ, SOM, and the proposed method were 99.00%, 99.24%, 98.74%, 98.00%, and 98.99% for accuracy, sensitivity, precision, Jaccard, and F1 score, respectively. In terms of compared methods, the proposed method was the most accurate because, when the GWO algorithm was used with feature selection, the accuracy increased to 99.00%.

A sample of the fault detection system is shown in Figure 9.

As seen in Figure 9, the a-g fault was given to the system, and the neural network correctly found this fault. First, the features of this signal were extracted, then the GWO algorithm was used to find the best and most suitable features to be used in the input of the neural network. Then, the trained neural network decided the fault type regarding the selected features. The model was tested many times and created the confusion matrix shown in Figure 6.

The faulted signals' varying fault resistances were tested, and the features were extracted from different resistance values. Furthermore, the input signals were fixed, and only the resistances were changed, and the scenarios of the faults were modified to extract

the features from the signals. In this study, the computational and hardware requirement of this algorithm, considering the time required to clear the fault, were not analyzed.

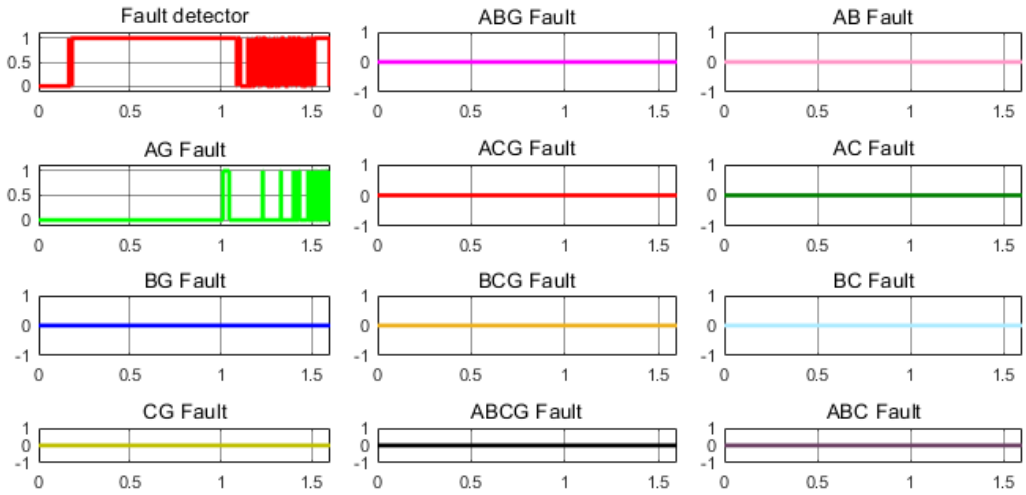

Figure 9. a-g Fault detected.

In this study, the classification performance of the proposed network was tested using a system that met the International Electrotechnical Commission standard. The analysis was done using MATLAB/Simulink; the discussion and the results are shown below. The explanation, the detailed results obtained, and the study's observations under specific conditions can also be listed accordingly when the figures are used in thesis work. The transformation device was used with power electronic devices during this converter simulation in order to compare the outcomes of this analysis.

The voltage, current signals, and alpha order results are shown in Figure 10.

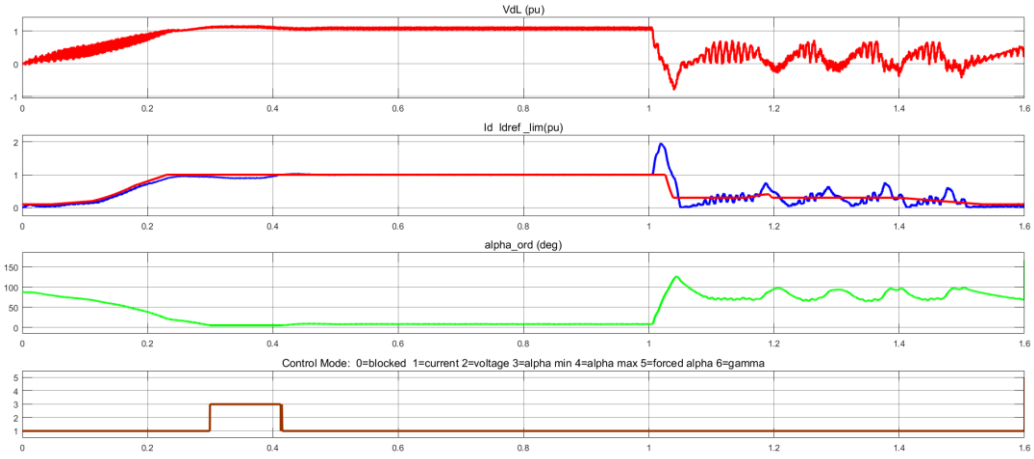

Figure 10. The voltage and the current signal, and alpha order.

This simulation results' control mode was arranged as 0, 1, 2, 3, 4, 5, and 6 for blocked case, current, voltage, alpha minimum, alpha maximum, forced alpha, and gamma. The three-phase voltage and current are shown in Figure 11.

As seen in Figure 11, the faulted signal occurred in the first second of the simulation. In Figure 11, the (X) axis shows the simulation time, and the (Y) axis shows the voltage and current amplitude value.

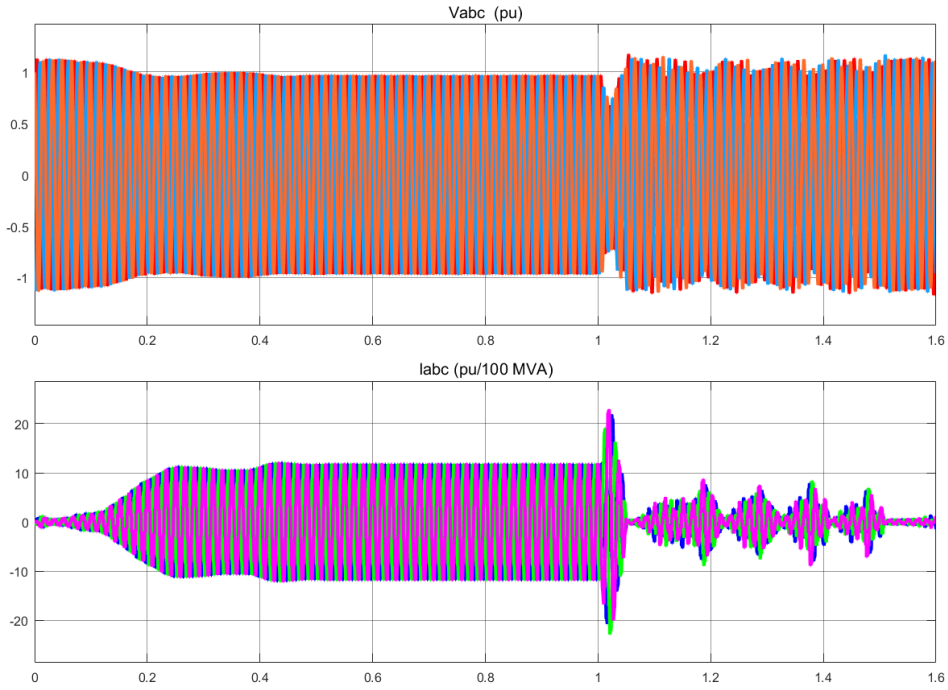

Figure 11. Three-phase voltage and current signals.

Figure 12 shows the reliable state condition at the rectifier section without any abnormal behavior in DC.

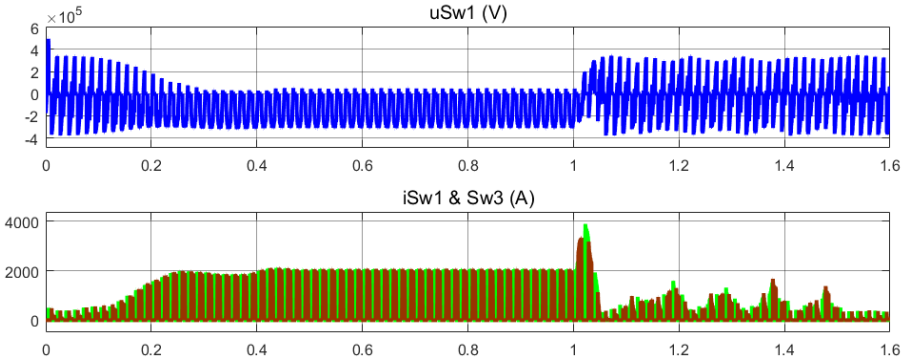

Figure 12. The reliable state condition at the rectifier section without any abnormal DC behavior.

As seen in Figure 12, the voltage and current signals did not have any faults. These signals were used to train ANN as non-faulted signals. In Figure 12 (as mentioned before), the (X) axis shows the simulation time, and the (Y) axis shows the amplitude value of the voltage and current.

Figure 13 demonstrates no faults at the rectifier (transmitting point) or the inverter (receiving point). The data displayed in Figure 12 represents current and voltage. This diagram makes it quite evident that at a time t = 1 s, the voltage was not naturally steady at the rectifier side. The voltage at the side of the inverter, which was the receiving point, stabilized, or became constant, after some time had passed or elapsed, as can be properly seen or observed. With a slight delay, the voltage and current values at the receiving point and at the inverter were nearly identical to those at the transmitting point, which was the rectifier side, unlike the transmitting and receiving points.

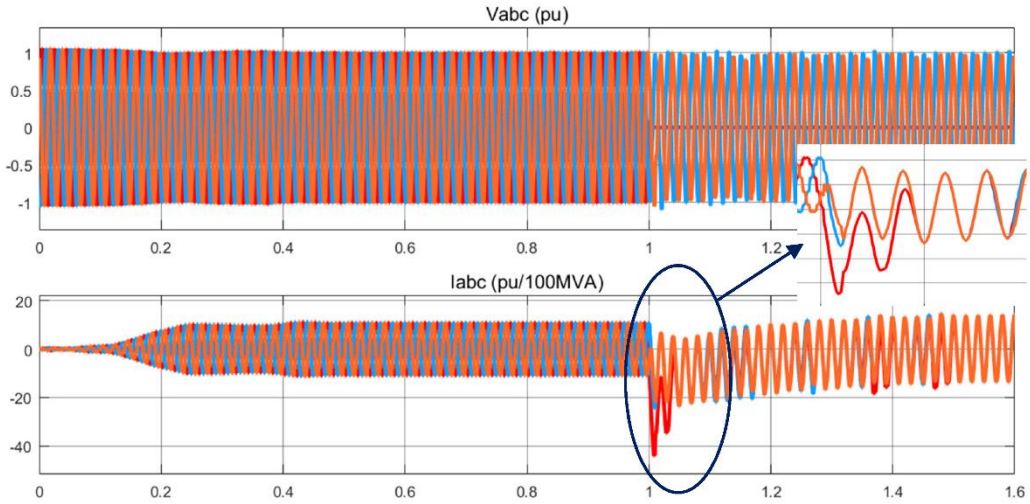

Figure 13. The absence of fault at both converters in three-phase voltage and current signals.

Figure 14 shows the faulted signal after 1 s at the rectifier (the transmitting point) and the inverter (the receiving point).

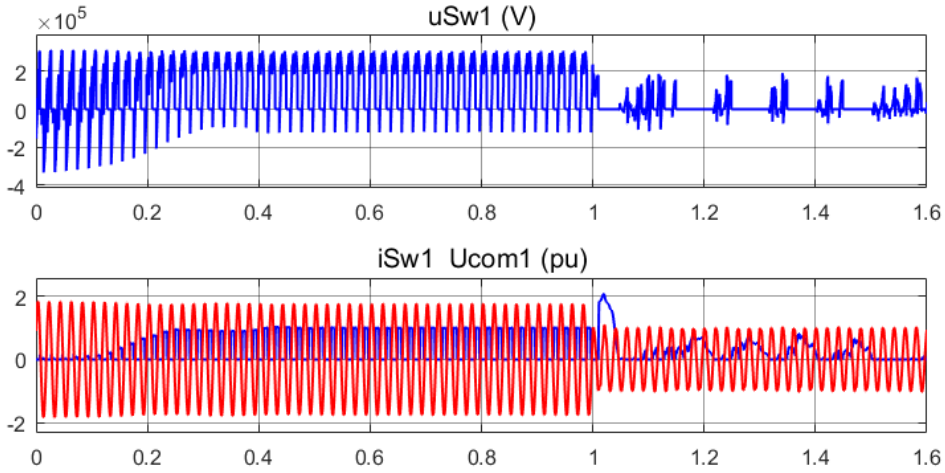

Figure 14. The faulted signal after 1 s at both rectifier (transmitting point) and inverter (receiving point).

The inverter malfunction produced an increase in the DC current Idc = 5.3 pu, while decreasing the DC voltage to Vdc = 0.5 pu. This further condition showed how a commutation failure can be readily caused by a fall in inverter voltage and an increase in current and how it can affect the stability of the AC grid supply.

6. Conclusions

In this paper, using the main characteristics measured on one side of the transmission line, based on voltage and current, an algorithm for fault detection in HVDC lines is proposed. In the proposed algorithm, when the start unit of the protection function in the protection system confirms the existence of a fault, the fault detection method uses the correlation level of voltage and fault current signals based on trained neural networks. In this study, firstly, the voltage and current signals are produced, which are used as feature signals. The GWO method is used to select the best and more effective features. The GWO algorithm selects the best features to train ANN. The GWO algorithm, based on ANN, can easily develop a fault locator with acceptable accuracy if a substantial quantity of data is used for training and learning. That is why the GWO algorithm, based on ANN, is becoming increasingly popular. This information was utilized to predict the results of unknown fault sites and different fault types simulated at various fault locations. For

future work, the authors recommend using different types of wavelets for feature extraction and different metaheuristic methods, such as the ant colony optimization method, Harris Hawks optimization, and particle swarm optimization, to find the different accuracy rates for fault detection scenarios.

Author Contributions: Conceptualization, R.S.J.; Methodology, R.S.J.; Software R.S.J.; Validation, H.A.; Investigation R.S.J.; Writing—original draft preparation, R.S.J.; Writing—review and editing, H.A.; Visualization, R.S.J.; Supervision, H.A. All authors have read and agreed to the published version of the manuscript.

Funding: This research received no external funding.

Data Availability Statement: No data were used to support this study.

Acknowledgments: We thank University of Sfax/ENIS for supporting this work.

Conflicts of Interest: The authors declare that there is no conflict of interest regarding the publication of this paper.

References

1. Liu, J.; Tai, N.; Fan, C.; Huang, W. Protection Scheme for High-voltage Direct-current Transmission Lines Based on Transient AC Current. *IET Gener. Transm. Distrib.* **2015**, *9*, 2633–2643. [CrossRef]
2. Zhang, Y.; Li, Y.; Song, J.; Li, B.; Chen, X.; Zeng, L. Novel Protection Scheme for High-voltage Direct-current Transmission Lines Based on One-terminal Transient AC Voltage. *J. Eng.* **2019**, *2019*, 4480–4485. [CrossRef]
3. Ahmadi, M.; Adewuyi, O.B.; Danish, M.S.S.; Mandal, P.; Yona, A.; Senjyu, T. Optimum Coordination of Centralized and Distributed Renewable Power Generation Incorporating Battery Storage System into the Electric Distribution Network. *Int. J. Electr. Power Energy Syst.* **2021**, *125*, 106458. [CrossRef]
4. Impram, S.; Nese, S.V.; Oral, B. Challenges of Renewable Energy Penetration on Power System Flexibility: A Survey. *Energy Strateg. Rev.* **2020**, *31*, 100539. [CrossRef]
5. Jordehi, A.R. Optimisation of Demand Response in Electric Power Systems, a Review. *Renew. Sustain. Energy Rev.* **2019**, *103*, 308–319. [CrossRef]
6. Baptista, I. Electricity Services Always in the Making: Informality and the Work of Infrastructure Maintenance and Repair in an African City. *Urban Stud.* **2019**, *56*, 510–525. [CrossRef]
7. Kandil, N.; Sood, V.K.; Khorasani, K.; Patel, R. V Fault Identification in an AC-DC Transmission System Using Neural Networks. *IEEE Trans. Power Syst.* **1992**, *7*, 812–819. [CrossRef]
8. Narendra, K.G.; Sood, V.K.; Khorasani, K.; Patel, R. Application of a Radial Basis Function (RBF) Neural Network for Fault Diagnosis in a HVDC System. *IEEE Trans. Power Syst.* **1998**, *13*, 177–183. [CrossRef]
9. Etemadi, H.; Sood, V.K.; Khorasani, K.; Patel, R.V. Neural Network Based Fault Diagnosis in an HVDC System. In Proceedings of the DRPT2000, International Conference on Electric Utility Deregulation and Restructuring and Power Technologies, (Cat. No. 00EX382), London, UK, 4–7 April 2000; pp. 209–214.
10. Shang, L.; Herold, G.; Jaeger, J.; Krebs, R.; Kumar, A. High-Speed Fault Identification and Protection for HVDC Line Using Wavelet Technique. In Proceedings of the 2001 IEEE Porto Power Tech Proceedings (Cat. No. 01EX502), Porto, Portugal, 10–13 September 2001; Volume 3, p. 5.
11. Gaouda, A.M.; El-Saadany, E.F.; Salama, M.M.A.; Sood, V.K.; Chikhani, A.Y. Monitoring HVDC Systems Using Wavelet Multi-Resolution Analysis. *IEEE Trans. Power Syst.* **2001**, *16*, 662–670. [CrossRef]
12. Gang, W.; Min, W.; Haifeng, L.; Chao, H. Transient Based Protection for HVDC Lines Using Wavelet-Multiresolution Signal Decomposition. In Proceedings of the 2005 IEEE/PES Transmission & Distribution Conference & Exposition: Asia and Pacific, Dalian, China, 18 August 2005; pp. 1–4.
13. Mei, J.; Ge, R.; Liu, Z.; Zhan, X.; Fan, G.; Zhu, P.; Chen, W. An Auxiliary Fault Identification Strategy of Flexible HVDC Grid Based on Convolutional Neural Network with Branch Structures. *IEEE Access* **2020**, *8*, 115922–115931. [CrossRef]
14. Liu, C.; Zhuo, F.; Wang, F. Fault Diagnosis of Commutation Failure Using Wavelet Transform and Wavelet Neural Network in HVDC Transmission System. *IEEE Trans. Instrum. Meas.* **2021**, *70*, 1–8. [CrossRef]
15. Wang, Q.; Yu, Y.; Ahmed, H.O.A.; Darwish, M.; Nandi, A.K. Open-Circuit Fault Detection and Classification of Modular Multilevel Converters in High Voltage Direct Current Systems (MMC-HVDC) with Long Short-Term Memory (LSTM) Method. *Sensors* **2021**, *21*, 4159. [CrossRef] [PubMed]
16. Wang, Y.; Zheng, D.; Jia, R. Fault Diagnosis Method for MMC-HVDC Based on Bi-GRU Neural Network. *Energies* **2022**, *15*, 994. [CrossRef]
17. Wang, Q.; Yu, Y.; Ahmed, H.O.A.; Darwish, M.; Nandi, A.K. Fault Detection and Classification in MMC-HVDC Systems Using Learning Methods. *Sensors* **2020**, *20*, 4438. [CrossRef] [PubMed]

18. Kar, S.; Samantaray, S.R.; Zadeh, M.D. Data-Mining Model Based Intelligent Differential Microgrid Protection Scheme. *IEEE Syst. J.* **2015**, *11*, 1161–1169. [CrossRef]
19. Ray, P.K.; Mohanty, S.R.; Kishor, N. Disturbance Detection in Grid-Connected Distributed Generation System Using Wavelet and S-Transform. *Electr. Power Syst. Res.* **2011**, *81*, 805–819. [CrossRef]
20. Mishra, M.; Rout, P.K. Detection and Classification of Micro-grid Faults Based on HHT and Machine Learning Techniques. *IET Gener. Transm. Distrib.* **2018**, *12*, 388–397. [CrossRef]
21. Manohar, M.; Koley, E.; Ghosh, S. Microgrid Protection under Wind Speed Intermittency Using Extreme Learning Machine. *Comput. Electr. Eng.* **2018**, *72*, 369–382. [CrossRef]
22. Hong, Y.-Y.; Cabatac, M.T.A.M. Fault Detection, Classification, and Location by Static Switch in Microgrids Using Wavelet Transform and Taguchi-Based Artificial Neural Network. *IEEE Syst. J.* **2019**, *14*, 2725–2735. [CrossRef]
23. Fahim, S.R.; Datta, D.; Sheikh, M.D.R.I.; Dey, S.; Sarker, Y.; Sarker, S.K.; Badal, F.R.; Das, S.K. A Visual Analytic in Deep Learning Approach to Eye Movement for Human-Machine Interaction Based on Inertia Measurement. *IEEE Access* **2020**, *8*, 45924–45937. [CrossRef]
24. Sarker, Y.; Fahim, S.R.; Sarker, S.K.; Badal, F.R.; Das, S.K.; Mondal, M.N.I. A Multidimensional Pixel-Wise Convolutional Neural Network for Hyperspectral Image Classification. In Proceedings of the 2019 IEEE International Conference on Robotics, Automation, Artificial-Intelligence and Internet-of-Things (RAAICON), Dhaka, Bangladesh, 29 November–1 December 2019; pp. 104–107.
25. Fahim, S.R.; Sarker, Y.; Rashiduzzaman, M.; Islam, O.K.; Sarker, S.K.; Das, S.K. A Human-Computer Interaction System Utilizing Inertial Measurement Unit and Convolutional Neural Network. In Proceedings of the 2019 5th International Conference on Advances in Electrical Engineering (ICAEE), Dhaka, Bangladesh, 26–28 September 2019; pp. 880–885.
26. Ab-BelKhair, A.; Rahebi, J.; Abdulhamed Mohamed Nureddin, A. A Study of Deep Neural Network Controller-Based Power Quality Improvement of Hybrid PV/Wind Systems by Using Smart Inverter. *Int. J. Photoenergy* **2020**, *2020*, 8891469. [CrossRef]
27. Nureddin, A.A.M.; Rahebi, J.; Ab-BelKhair, A. Power Management Controller for Microgrid Integration of Hybrid PV/Fuel Cell System Based on Artificial Deep Neural Network. *Int. J. Photoenergy* **2020**, *2020*, 8896412. [CrossRef]
28. Mirjalili, S.; Mirjalili, S.M.; Lewis, A. Grey Wolf Optimizer. *Adv. Eng. Softw.* **2014**, *69*, 46–61. [CrossRef]
29. Gurney, K. *An Introduction to Neural Networks*; CRC Press: Boca Raton, FL, USA, 2018; ISBN 1315273578.
30. Fernández-Montoya, J.; Avendaño, C.; Negredo, P. The Glutamatergic System in Primary Somatosensory Neurons and Its Involvement in Sensory Input-Dependent Plasticity. *Int. J. Mol. Sci.* **2018**, *19*, 69. [CrossRef]
31. Tran, T.T.K.; Bateni, S.M.; Ki, S.J.; Vosoughifar, H. A Review of Neural Networks for Air Temperature Forecasting. *Water* **2021**, *13*, 1294. [CrossRef]
32. Zhang, T.; Li, C.; Liang, J. A Thyristor Based Series Power Flow Control Device for Multi-Terminal HVDC Transmission. In Proceedings of the 2014 49th International Universities Power Engineering Conference (UPEC), Cluj-Napoca, Romania, 2–5 September 2014; pp. 1–5.
33. Candelaria, J.; Park, J.-D. VSC-HVDC System Protection: A Review of Current Methods. In Proceedings of the 2011 IEEE/PES Power Systems Conference and Exposition, Phoenix, AZ, USA, 20–23 March 2011; pp. 1–7.
34. Swetapadma, A.; Agarwal, S.; Chakrabarti, S.; Chakrabarti, S.; El-Shahat, A.; Abdelaziz, A.Y. Locating Faults in Thyristor-Based LCC-HVDC Transmission Lines Using Single End Measurements and Boosting Ensemble. *Electronics* **2022**, *11*, 186. [CrossRef]
35. Al-Rahlawee, A.T.H.; Rahebi, J. Multilevel Thresholding of Images with Improved Otsu Thresholding by Black Widow Optimization Algorithm. *Multimed. Tools Appl.* **2021**, *80*, 28217–28243. [CrossRef]
36. Albargathe, S.M.B.K.; Kamberli, E.; Kandemirli, F.; Rahebi, J. Blood Vessel Segmentation and Extraction Using H-Minima Method Based on Image Processing Techniques. *Multimed. Tools Appl.* **2021**, *80*, 2565–2582. [CrossRef]
37. Mohamed, A.A.I.; Ali, M.M.; Nusrat, K.; Rahebi, J.; Sayiner, A.; Kandemirli, F. Melanoma Skin Cancer Segmentation with Image Region Growing Based on Fuzzy Clustering Mean. *Int. J. Eng. Innov. Res.* **2017**, *6*, 91–95.